Paper No. 531. (quote when citing this article)
Eleventh World Conference on Earthquake Engineering
ISBN: 0 08 042822 3

SEISMIC BEHAVIOR OF EMBANKMENT PLACED ON SATURATED SANDS

NAOTO OHBO[1], JINGZHE ZHENG[1], KAZUO YOSHIZAKO[1], NOBUO MISHIMA[2], KAZUYUKI NAGAO[2] and TOMOYUKI BETSUI[2]

1)Civi Engineering Department I, Kajima Technical Research Institute, Kajima Corporation, 19-1, Tobitakyu 2-Chome, Chofu-shi, Tokyo 182, Japan
2)Japan Highway Public Corporation, 1-4-1, Tadao, Machida-shi, Tokyo 194, Japan

ABSTRACT

This paper investigates the seismic behavior of embankment placed on saturated sands during large earthquakes through analysis and simulation of dynamic centrifuge tests. The TOMEI highway embankment is selected for investigation, and three kinds of underlying sand conditions (Dr=39%, 56%, 93%) are considered. The results of centrifuge tests are first analyzed, and then the numerical simulation are performed using 2-phase nonlinear FEM. The mechanism of embankment failure due to soil liquefaction is interpreted with aid of numerical model, and the discussion on countermeasure against liquefaction is conducted.

KEYWORDS

Highway embankment; liquefaction; centrifuge test; 2D FEM; 2-phase nonlinear analysis.

INTRODUCTION

Recently, many embankment damages due to liquefaction of underlying soil during earthquakes have been reported (e.g., JSCE, 1986), which results in a great demand to comprehend the seismic behavior of embankment under various conditions and develop effective countermeasure against soil liquefaction. During these years, experimental studies and numerical analysis (Koseki, 1983; Abe and Kusano, 1992) have been conducted to investigate the seismic behavior of embankment resting upon saturated sands, which have demonstrated the effects of the underlying soil conditions, the embankment conditions and the characteristics of seismic motions. However, to understand the mechanism of embankment failure due to soil liquefaction under various conditions, further studies are required because of the limited number of previous studies and the difficulties of the problem.

This paper investigates the seismic behavior of a highway embankment resting on saturated sands through the simulation and analysis of dynamic centrifuge tests. Three kinds of underlying saturated sands (Dr=39%, 56%, 93%) are considered. The test results are first simulated and analyzed using two-phase nonlinear FEM, and then the mechanism of embankment failure due to soil liquefaction is studied using validated numerical model. In addition, the discussion on countermeasures against liquefaction is conducted.

CENTRIFUGE TESTS AND NUMERICAL MODEL

Centrifuge tests

Three centrifuge model experiments have been carried out at 50g centrifugal acceleration. The standard cross section of TOMEI highway embankment has been adopted as that of embankment model. The cross section of experiment model together with arrangement of measuring apparatus are shown in Fig. 1. The embankment has been assumed to be placed on saturated sands, and three different sand conditions with relative density of 39%, 56% and 93% have been considered. The test model has been constructed and tested in following way. The Toyoura standard sand is first drily pluviated into a rigid box, and the sands are saturated using silicone oil. The embankment is modeled using Toyoura sand mixed with Kaolin clay, the ratio between sand and clay is 5:1. Silicone rubber is set between sand and end walls to reduce the effects of end walls. The rigid box is set on the platform of shaker, and sinusoidal acceleration of 200Hz with amplitude of around 10g is applied at the bottom of rigid box. Pore water pressure transducers, accelerometers and linear variable differential transformers (LVDT) are set up to observe the response of embankment and underlying sands. The test conditions are shown in Table 1.

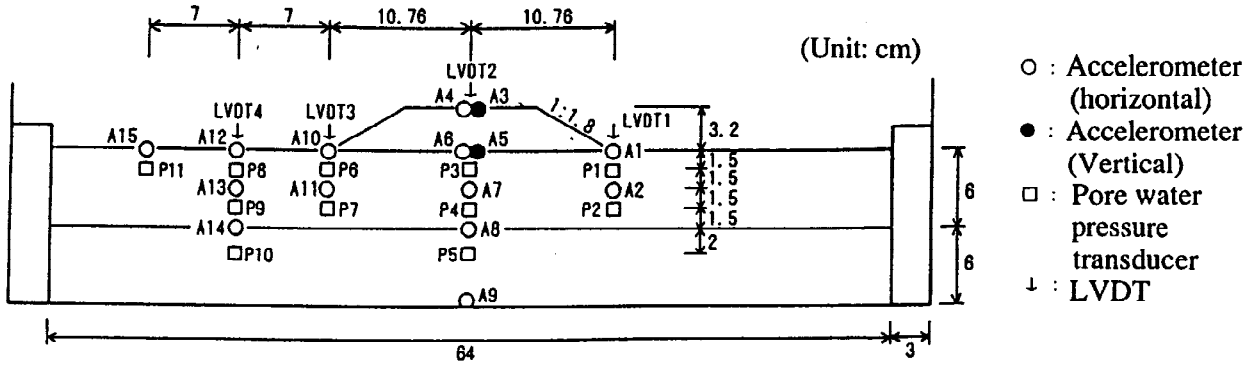

Fig. 1. Outline of centrifuge test.

Table 1. Centrifuge test condition

Model test	Base motion	A_{max} (g)	Depth of sands (cm)	Relative density of sands (%)
A	Sinusoidal	9.1	11.48	39
B	Sinusoidal	9.5	11.82	56
C	Sinusoidal	7.9	11.87	93

Table 2. Model constitutive parameters

Constitutive parameter	Symbol
Mass density — solid	ρ_s
Porosity	n^w
Low-strain shear and bulk moduli	G_0, B_0
Reference mean effective normal stress	p_0
Power exponent	n
Friction angle at failure	ϕ
Cohesion	c
Maximum deviatoric strain	ϵ_{dev}^{max}
Dilation angle	$\bar{\phi}$
Dilation parameter (cyclic)	X_{pp}
Permeability	k

Numerical model

The 2-phase nonlinear finite element code DYNAFLOW (Prevost, 1981) is used for numerical analysis. Figure 2 shows the finite element model. The multi-yield constitutive soil model is adopted (Prevost, 1985) to simulate the nonlinear behavior of the soil materials. Table 2 demonstrates all the required parameters, which can be derived from the results of conventional laboratory tests.

To find the model parameters, triaxial soil tests and undrained cyclic triaxial soil tests are performed, based on which the material parameters for sands with different relative density and embankment material are determined. Table. 3 shows the material parameters for sands and embankment material. Figure 3 represents computed and observed liquefaction strength for the case when relative density is 56%.

The calculation is performed in two steps. First, consolidation under gravity loads is calculated. After the consolidation is completed, the nodal displacement, velocity and acceleration are set to zero, and the dynamic loads are applied.

Table. 3 Material parameters for sands and embankment material

Property	Sands			Embankment material
	Dr=39%	Dr=56%	Dr=93%	
Solid mass density(kg/m^3)	2648.0	2648.0	2648.0	2683.0
Porosity	0.455	0.436	0.388	0.390
Initial shear modulus(MPa)	85.5	97.1	129.7	86.0
Initial bulk modulus(MPa)	185.2	195.5	281.0	401.1
Reference mean stress(kPa)	98.0	98.0	98.0	98.0
Power exponent	0.4	0.4	0.4	0.3
Fluid bulk modulus(MPa)	2000.0	2000.0	2000.0	-
Friction angle at failure(deg.)	36.8	38.4	44.0	27.0
Cohesion(kPa)	0.0	0.0	0.0	1.0
Maximum deviatoric strain(%)	7.0	6.0	5.0	7.0
Dilation angle(deg.)	30.0	30.0	30.0	27.0
Dilation parameter	0.21	0.15	0.10	-
Permeability(m/s)	6.0E-05	5.0E-05	4.0E-05	-

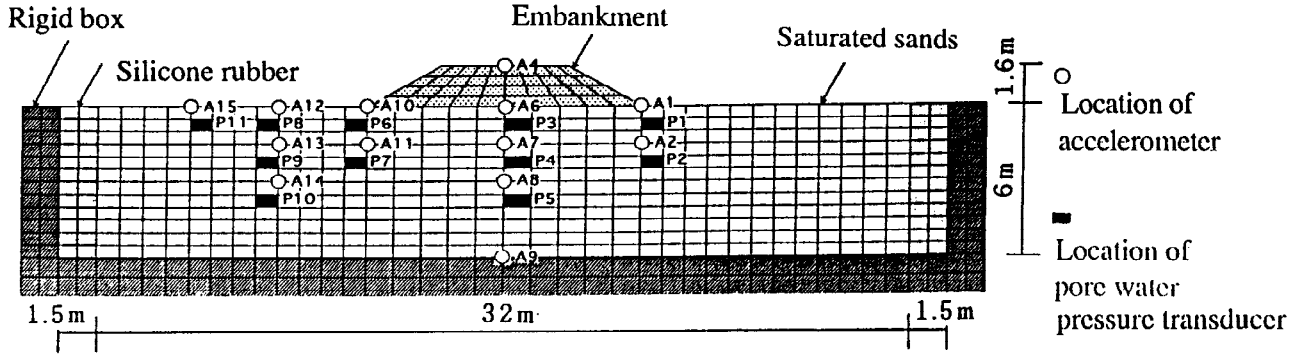

Fig. 2. FEM model in prototype term

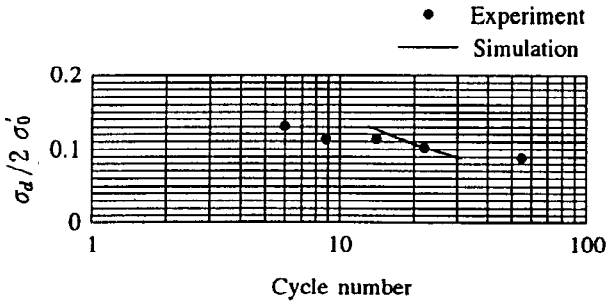

Fig. 3. Liquefaction strength curve

NUMERICAL RESULTS AND DISCUSSION

The observed and computed acceleration responses at A15 and A1, and excess pore water pressures at P11 and P1 for the cases with relative density of 39%, 56% and 93% are presented in Fig. 4, Fig. 5 and Fig.6, respectively. The settlements of embankment in three cases are shown in Fig. 7. All results are presented in prototype terms. It could be seen that the computed results match well with the observed ones both in magnitude of amplitude and waveform. Good agreement between computed and observed responses is also confirmed at all other observing points, which demonstrates the validity of the presented numerical model.

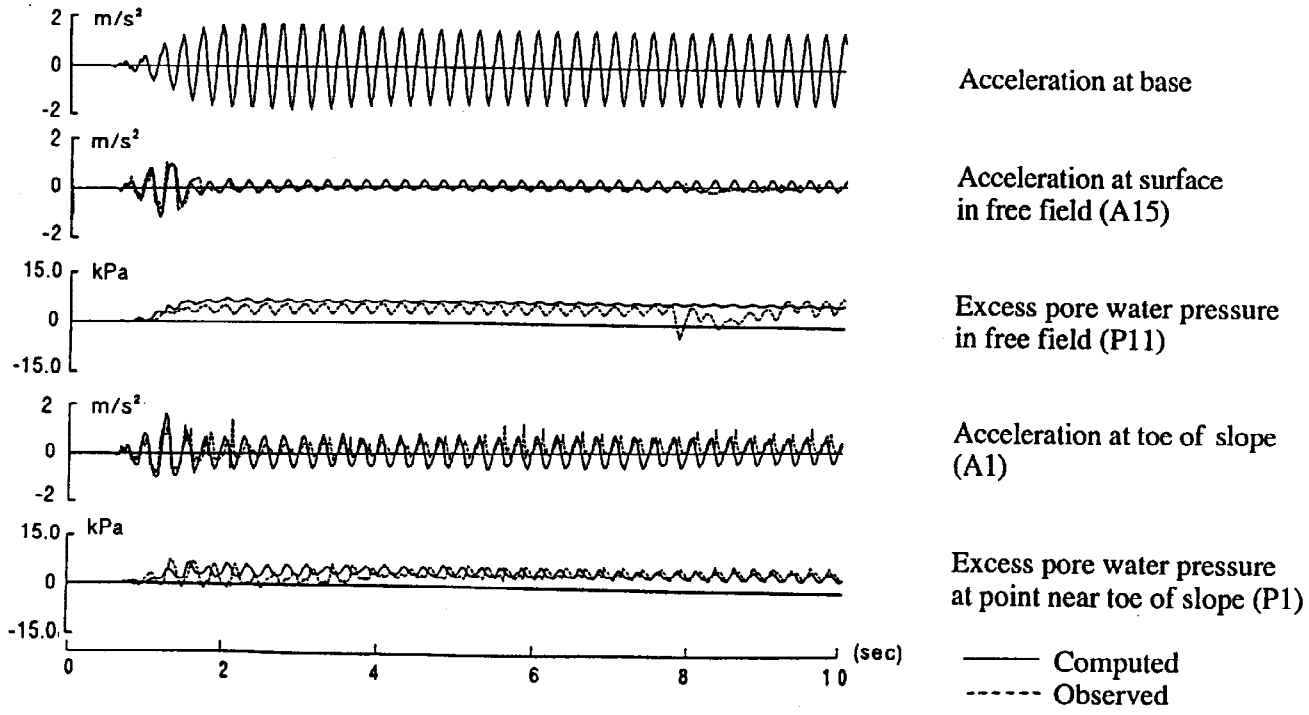

Fig. 4. Computed and observed accelerations and excess pore water pressures (Dr=39%)

In the region that is relatively far from the embankment (hereafter called free filed), as the amplitude of acceleration increases, the excess pore water pressure begins to rise, and soon reaches the maximum value. The amplitude of acceleration quickly decreases as the excess pore water pressure increases, and shows very small amplitude after the excess pore water pressure arrives its maximum. The maximum excess pore water pressure ratios in all three cases are greater than 0.9, indicating that the sand ground liquefies.

At the observing point at the toe of the slope of embankment, the reduction of amplitude of acceleration is not as significant as observed in free field. The maximum excess pore water pressure ratio at this point is less than 0.8, indicating that the sand ground under and near embankment does not liquefy (refer also to Fig. 8, 9, 10), and thus the reduction of amplitude of acceleration is smaller compared with that in free field. This may result from the fact that the effective vertical stress in sand ground under embankment is higher than those in free filed due to the weight of embankment. The wave form of excess pore water pressure is also different from that at observing points in free field, which reflects the effects of embankment on the dynamic response characteristics of its surrounding sands.

As for the effects of relative density of underlying sands, low density leads to fast generation of excess pore water pressure and quick reduction of amplitude of acceleration, as shown in Fig. 4, Fig.5 and Fig. 6. It could also be seen that the settlement of embankment in the case with low relative density is significantly large, as reflected in Fig. 7. These could be explained as following. Compared with the sand of high relative density, the sand with low relative density has lower liquefaction strength, and thus is easier to liquefy, and the liquefied zone is also larger (refer to Fig. 8,9,10), which results in more significant settlement of embankment.

Figure 8, 9 and 10 demonstrate the distribution of excess pore water pressure ratio and horizontal normal effective stress after sand ground liquefies for the cases with relative density of 39%, 56% and 93%, respectively. The sand ground in free field liquefies, while the sand ground beneath and near embankment do not. It can also be seen that low relative density results in large liquefied region. Regarding the horizontal normal effective stress, tensile stress could be found in the part near the surface of embankment, which implies that the crack may occur in these region. In the centrifuge tests, the cracks occurred at the surface of embankment in the direction perpendicular to the embankment section. Therefore, the results shown in Fig. 8, Fig. 9 and Fig.10 well explain the test results. The mechanism of the tensile stress generation is as following. When the sand ground in free field liquefies, the sand ground beneath embankment horizontally extends towards the free field due to the weight of embankment. Thus, the embankment is horizontally pulled by the

extending of underlying sand ground. When the tensile stress generated by the extending of underlying sand exceeds the compressive stress due to self-weight of embankment, the whole effective stress becomes tensile, which could lead to the occurring of cracks if it exceeds the tensile strength of embankment materials.

Therefore, the pattern of embankment failure due to soil liquefaction is that embankment settles together with cracks occurring in direction perpendicular to embankment section due to the horizontal extension of underlying sand ground. This pattern well agrees the results of many experiments and earthquake damage reports (e.g., Nagao *et al.*, 1986; JSCE, 1986).

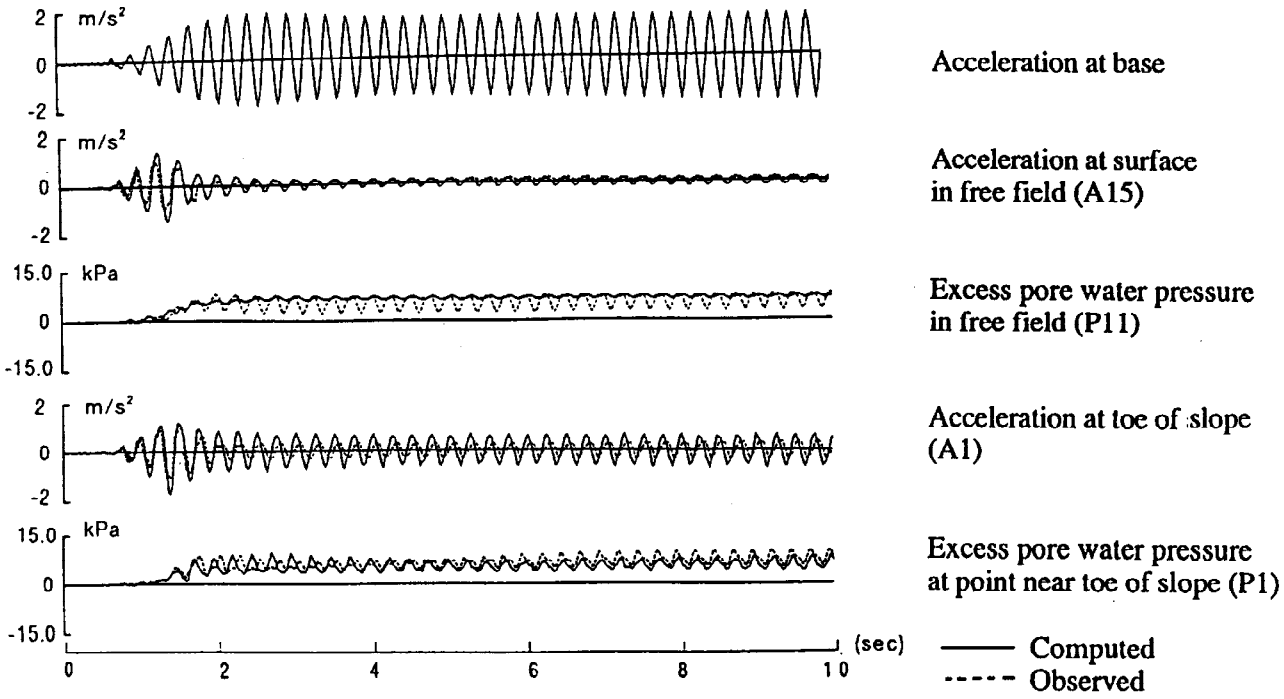

Fig. 5 Computed and observed accelerations and excess pore water pressures (Dr=56%)

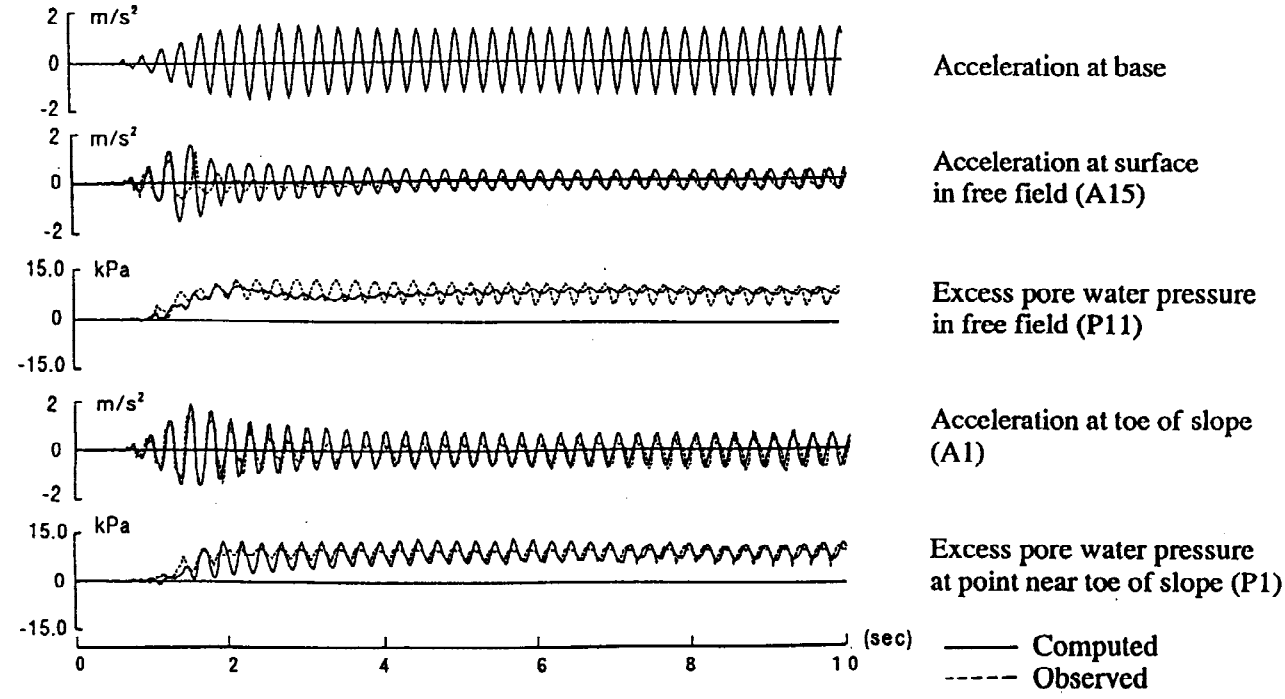

Fig. 6. Computed and observed accelerations and excess pore water pressures (Dr=93%)

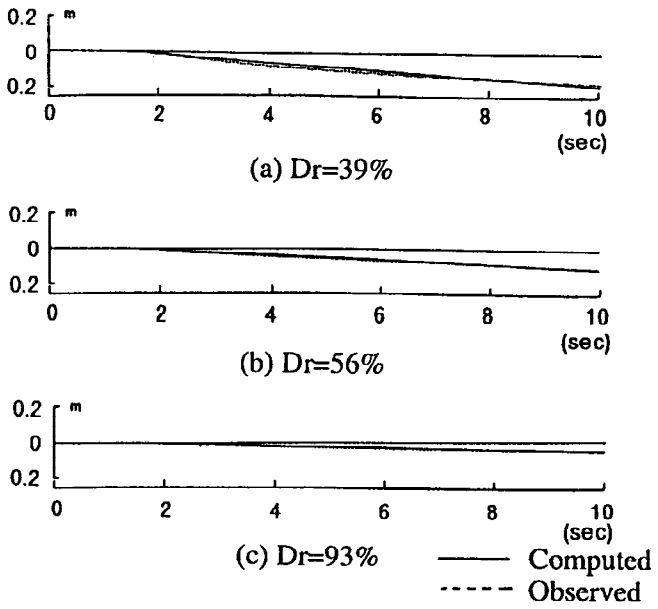

Fig. 7. Computed and observed settlement of embankment

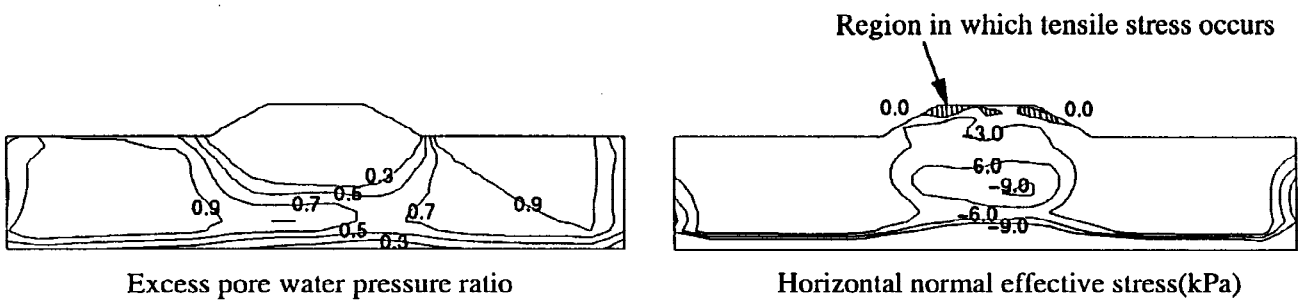

Fig. 8. Distribution of excess pore water pressure ratio and horizontal normal effective stress(Dr=39%)

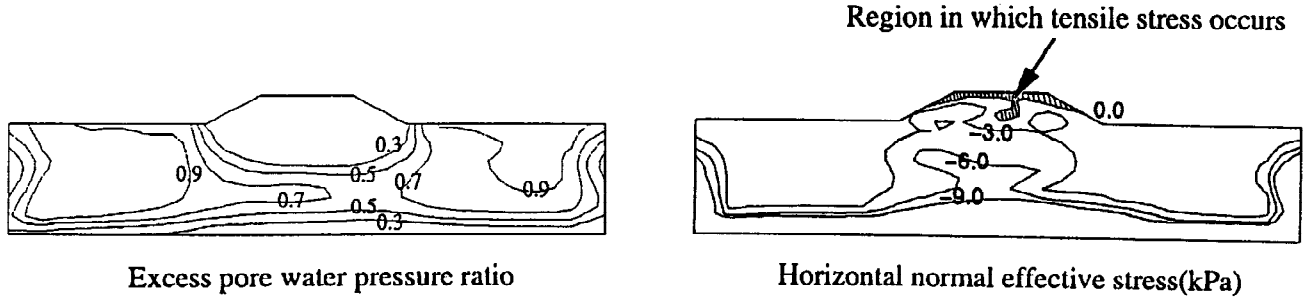

Fig. 9. Distribution of excess pore water pressure ratio and horizontal normal effective stress(Dr=56%)

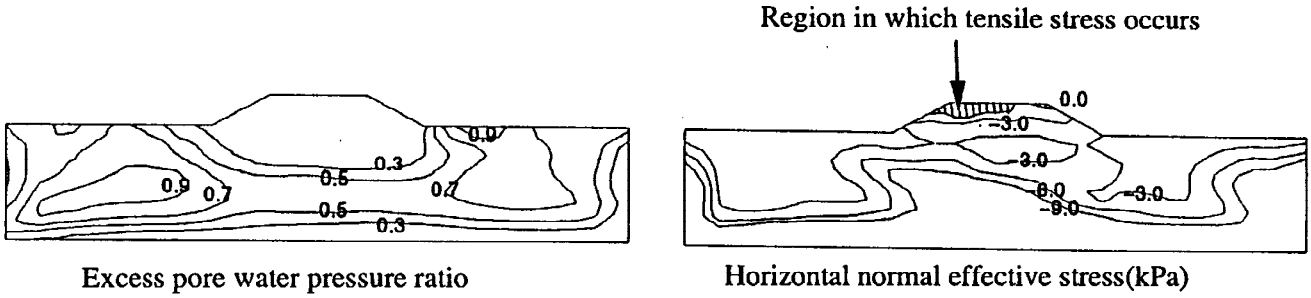

Fig. 10 Distribution of excess pore water pressure ratio and horizontal normal effective stress (Dr=93%)

DISCUSSION ON COUNTERMEASURE

From the above results, it could be concluded that, for the prevention of embankment damage, it is important to constrain the horizontal extending of sand ground under embankment. Thus, to increase the strength of the soil just under the toe of slope of embankment, or to directly constrain the soil under embankment could be promising countermeasures. If only the prevention of cracking in embankment is of importance, to directly reinforce the horizontal deformation of embankment may be economic effective method. In this study, following two countermeasures are chosen for evaluation. One is a countermeasure using counterweight-fill (hereafter called countermeasure A), which is aimed at improving the soil condition around the toe of slope. The other is a countermeasure using steel-wire-net (hereafter called countermeasure B), which is only for constraining the horizontal deformation of embankment. In both cases, the underlying sands and input wave are assumed to be exactly the same as those in case B (Dr=56%) as shown in Table 1. Figure 11 represents the FEM model for the case of countermeasure A. The material of embankment is used as that of counterweight-fill. As for the case of countermeasure B, beam elements with no bending rigidity are applied at the bottom of embankment to represent the steel-wire-net. The section of whole model is the same as that shown in Fig. 2.

Figure 12 and 13 demonstrate the distribution of excess pore water pressure ratio and horizontal stress after surrounding sands liquefies, for the cases of countermeasure A and B, respectively. Compared with the case without countermeasure (see Fig. 9), when using countermeasure A, the liqufied region (with excess pore water pressure ratio larger than 0.9) decreases, and the depth of tensioned region in embankment becomes shallow, and the area of tensioned area small, which clearly reflects the effects of counterweight-fill. In the case with countermeasure B, the distribution of liquefied region is almost the same as that in the case without countermeasure, indicating the reinforcement of embankment has almost no effects on the behavior of underlying sands. However, the depth and area of tensioned region in embankment are smaller than those in the case without countermeasure, demonstrating that the steel-wire-net constrain the horizontal deformation of embankment. As for the settlement of embankment, the results in above three cases are almost the same. Therefore, both countermeasure A and countermeasure B reduce the tensioned region in embankment, but seem to have little effects on the settlement of embankment.

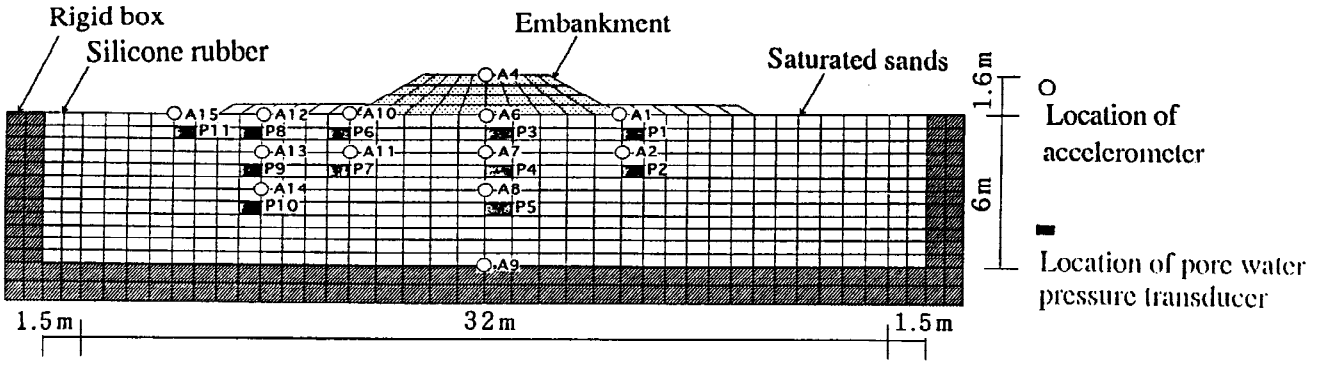

Fig. 11. FEM model for case using counterweight-fill

CONCLUSIONS

To study the behavior of highway embankment resting upon saturated sands, the results of dynamic centrifuge tests are simulated and analyzed using 2-phase nonlinear FEM. Using the validated numerical model, the mechanism of embankment failure due to soil liquefaction is studied, and the countermeasure against soil liquefaction is discussed. Following are the main conclusions drawn from this study: (1) The presented numerical model proves to be able of simulating the centrifuge tests, and providing substantial information for comprehending the centrifuge test results; (2)The excess pore water pressure ratios are considerably small in the region close to the bottom of embankment, and the soil under embankment is harder to liquefy compared with the sands in free-field; (3)The relative density of underlying sands has significant effects on the seismic behavior of embankment. Low relative density results in fast liquefaction and large liquefied region, and thus leads to large settlement of embankment; (4)The pattern of embankment failure is that embankment settles together with cracks occurring due to the horizontal extension of underlying sand ground. Both the countermeasure using counterweight-fill and that using steel-wire-net could reduce the tensioned region in embankment.

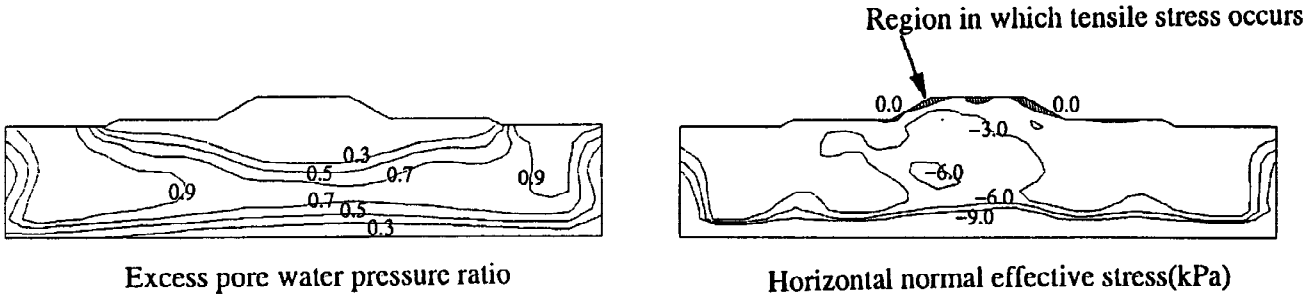

Fig. 12. Distribution of excess pore water pressure ratio and horizontal normal stress (Countermeasure A)

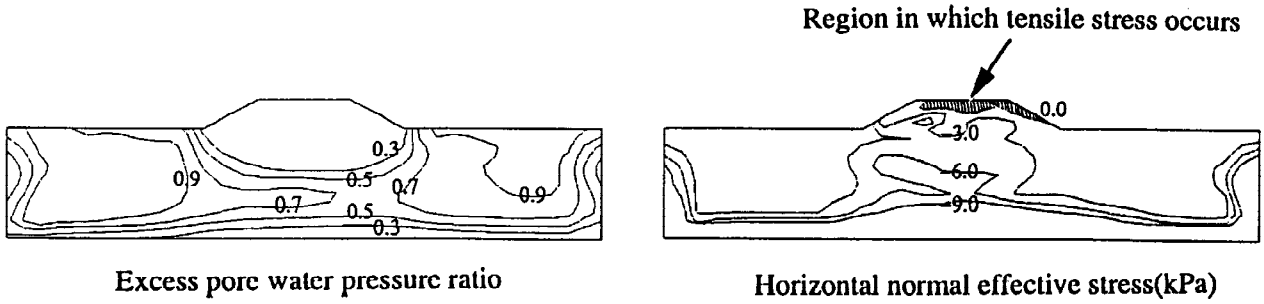

Fig. 13. Distribution of excess pore water pressure ratio and horizontal normal stress (Countermeasure B)

REFERENCE

Abe, H. and Y. Kusano(1992). Liquefaction analysis of embankment using 2D FEM. Proc. 46th Annual Conference of JSCE, **3**, 986-987. (in Japanese)

Koseki, J. (1983). Dynamic centrifuge tests on embankment placed on sandy ground. Proc. 24th Annual Conference of JSSMFE, 1123-1126. (in Japanese)

JSCE(1986). *Damage report of the Nion-kai Central Part Earthquake in 1983.* JSCE. (in Japanese)

Nagao, K. and T. Iriyama(1994). Effects of relative density of underlying sands on the behavior of embankment. Proc. 50th Annual Conference of JSCE, **3**, 96-97. (in Japanese)

Prevost, H.J.(1981).DYNAFLOW: A nonlinear transient finite element analysis program. Dept. Civil Engineering Op. Res., Princeton University. Last update 1994.

Prevost, H.J. (1985). A simple plasticity theory for fricional cohensionless soils. *J. Soil Dynam. Earthq. Eng.*, **4**, 9-17.